FLOW BOILING HEAT TRANSFER COEFFICIENT OF R-134a/R-290/R-600a MIXTURE IN A SMOOTH HORIZONTAL TUBE

by

Raja BALAKRISHNAN, Mohan Lal DHASAN, and Saravanan RAJAGOPAL

Original scientific paper
UDC: 66.045.1:536.24
BIBLID: 0354-9836. *12* (2008), 3, 33-44
DOI: 10.2298/TSCI0803033B

An investigation on in-tube flow boiling heat transfer of R-134a/R-290/R-600a (91%/4.068%/4.932% by mass) refrigerant mixture has been carried out in a varied heat flux condition using a tube-in-tube counter-flow test section. The boiling heat transfer coefficients at temperatures between –5 and 5 °C for mass flow rates varying from 3 to 5 g/s were experimentally arrived. Acetone is used as hot fluid, which flows in the outer tube of diameter 28.57 mm, while the test fluid flows in the inner tube of diameter 9.52 mm. By regulating the acetone flow rate and its entry temperature, different heat flux conditions between 2 and 8 kW/m^2 were maintained. The pressure of the refrigerant was maintained at 3.5, 4, and 5 bar. Flow pattern maps constructed for the considered operating conditions indicated that the flow was predominantly stratified and stratified wavy. The heat transfer coefficient was found to vary between 500 and 2200 W/m^{2}K. The effect of nucleate boiling prevailing even at high vapor quality in a low mass and heat flux application is highlighted. The comparison of experimental results with the familiar correlations showed that the correlations over predict the heat transfer coefficients of this mixture.

Key words: *flow boiling, heat transfer coefficient, stratified flow, acetone, R-134a, HC blend, M09*

Introduction

The chlorofluorocarbons (CFC) are to be phased out by 2010 as per Montreal Protocol [1]. The research and development efforts during the past decades have evolved R-134a and hydrocarbon blends as prominent substitutes for R-12 [2-5]. But if the existing R-12 systems are to be converted to work with R-134a, the compressor itself has to be changed as R-134a is immiscible with mineral oil. The matching oil for R-134a is polyol ester (POE) oil which is hygroscopic in nature and may cause moisture entry into the circuit during service and maintenance operations. On the other hand even though hydrocarbon blend is miscible with mineral oil, its flammable nature has caused concerns. Hence it is prudent to look for a refrigerant-oil pair that neither has service nor flammability issues.

It is reported in our earlier works [6, 7] that adding 9% of hydrocarbon blend to R-134a makes the resultant zeotropic mixture (M09) work well with mineral oil with enhanced performance. It can be a used as a drop-in-substitute for R-12. In this work the flow boiling heat transfer coefficient of this M09 in horizontal tube is studied for the conditions prevailing in the evap-

orator of a typical domestic refrigerator. The outcome of this work will form a basis for studies on enhanced tubes, mini channel, and correlation development for M09.

Flow boiling – low heat and mass flux applications

The flow boiling process in a low heat and mass flux application is closely related to flow patterns and suppression of nucleation. Further, the heat transfer coefficient so evolved also depends on the mode of heat transfer used in the experiments. It is prudent to review the existing literature related to these applications to understand the heat transfer coefficient and its mechanism.

Flow boiling heat transfer can be postulated based on the flow pattern prevailing inside a heated tube. Flow pattern is the topological self alignment of liquid and vapour inside a heated section which depend on the fluid characteristics, operating conditions, and flow orientation. There are more number of published literature available on experimentation of flow boiling heat transfer for annular flow pattern as compared to stratified flow pattern. Chen [8] hypothesized that in a typical annular flow boiling process, there exists two distinguished regions which are the nucleation dominant region and the convective dominant region. In the former the heat transfer is predominantly due to nucleation and in the latter it is due to convective vaporization of liquid at the liquid-vapor interface where the nucleation is considered to be absent. It has been pointed out that these regions can be demarcated by identifying the location where nucleation gets suppressed [9-11]. Jung *et al*. [9, 10], Shin *et al*. [11] and many other experimenters on refrigerants and mixtures have reported that a clear cut demarcating vapour quality can be realized between nucleate and convective boiling phenomenon in both mixture and pure fluids. It is also reported that in the convective region the heat transfer coefficients are independent of heat flux for a given pressure. For a given pressure and mass flow rate, the heat transfer coefficient lines for a range of heat flux merge into a single line once the nucleation is suppressed.

In the case of domestic refrigerators and freezers, for which the present study is intended, the heat flux and mass flux are low. The predominant flow patterns corresponding to these conditions are stratified and stratified-wavy flow [12, 13]. Stratified flow pattern differ from an annular pattern by the presence of an un-wetted perimeter and in stratified-wavy flow pattern, waves of flowing liquid splash on the top part of the tube and thus increases the wetted perimeter intermittently. It is reported that in the evaporator tubes of these conditions, unlike annular flow, the nucleation is not completely suppressed even at higher vapour qualities [12-14]. Wattelet *et al.* [12] conducted experiments on R-12, R-134a, and R-22/R-124/R-152a for stratified and stratified-wavy flow conditions in an electrically heated test section. It is reported that heat transfer coefficient is depended on heat flux through out the flow boiling process and the nucleation was not fully suppressed.

Jabardo *et al*. [13] performed experiments on R-22, R-404A, and R-134a using a 2 m electrically heated test section at 8 and 15 °C. It was reported that for conditions for low mass fluxes, the heat transfer coefficient through out the boiling regime was a strong function of heat flux. The heat transfer curve did not merge into a single line which indicated that the suppression of nucleation was absent. It was also reported that heat transfer coefficient at lower saturation temperature is higher than that at high saturation temperature. This behaviour is attributed to the fact that the thermal resistance of the film attached to the tube surface is inversely proportional to the thermal conductivity of the liquid. Since the conductivity of the liquid diminishes with temperature, so does the heat transfer coefficient.

Experiments of Aprea *et al*. [14] on R-22 and R-407C revealed that at low mass fluxes the heat transfer coefficient only slightly depended on forced convective effect. It is reported

that stratified-wavy flow is predominant in the evaporator. Therefore, both nucleation and liquid convection are active heat transfer mechanisms in the global heat transfer process.

Experiments of Ross *et al.* [15] on R-152a and R-13B1 (individually as well in mixed state) claimed that at high pressure (4.75 bar) the effect of nucleation was not dissipated at higher vapor qualities. But it can be also observed that when the pressure was lowered (around 1.5 bar) the nucleation was suppressed at a lower vapor quality and the heat transfer coefficient was dominated by convection. The heat transfer coefficient which is inversely proportional to wall super heat for a constant heat flux is found to be decreasing for higher pressure condition. This is an indication that at higher pressure the nucleation prevails through out the flow boiling process. It is needless to mention that in flow boiling the convective vaporization process results in higher heat transfer coefficient than the nucleation process.

It is to be noted that in most of the cases due to practical difficulty the length of the test section was always limited. Ross *et al*. [15] claimed that, applying high heat flux for a specified mass flux to attain at high vapor qualities in small test sections is not replicating the real conditions found in appliances. Shin *et al.* [11] claimed that it is not proper to use an electrically heated test section when the flow is stratified or tube is partially dried out. Jung *et al*. [9, 10] suggested that to study heat transfer coefficient of a refrigerant mixture more realistically, the preferred mode of heating would be a counter-current heat exchanger. Kattan *et al.* [16, 17] suggested that in a real time appliance the heat flux would never be constant and heat flux should not be imposed by the experimenter as done in electrically heated test sections. It is not a reasonable approximation to use a uniform heat flux for stratified and stratified-wavy flow patterns and the preferred mode of heating, especially for mixtures, would be through a counter current heat exchanger.

Most of the experimenters using electrically heated test section have limited the highest vapour quality to 80% to avoid tube burnout conditions. It is needless to say that in a typical evaporator the refrigerant enters the compressor either in a saturated vapour or in super heated state. Hence it is vital to study the complete vaporization process of any refrigerant.

Even though there are numerous correlations to predict the heat transfer coefficient which have come out of rigorous experimentation and analysis, it is true that familiar correlations are far deviating from actual in many cases. Shin *et al.* [11] studied the heat transfer characteristics of R-22, R-32, R-134a, R-32/R-134a, R-32/R-125, R-290, R-600a, and R-290/R-600a for annular flow conditions and have reported that Gungor *et al*. [18, 19] over-predicts the experimental results by around 30.5%. Aprea *et al*. [14] performed experiments using R-22 and R-407C for conditions which resemble a typical small scale refrigeration unit using a tube-in-tube test section and compared the same with familiar correlations. It is reported that correlations of Chen [8], Gungor *et al.* [18, 19], Shah [20], Kandlikar [21], and Kattan *et al.* [17] under predict heat transfer coefficient of R-22 and over predict that of R-407C.

In the present work a test section of 10 m length with a counter current heat exchanging arrangement is used to study the variation of heat transfer coefficient of M09 undergoing flow boiling by allowing complete vaporization ($x = 1$) under varied heat flux conditions. Thome [22] flow pattern map is used to identify the flow pattern for a given operating condition inside the heated channel. The significance of nucleation contribution at high vapour quality in a low mass and heat flux application is highlighted. The paper also compares the experimental results with Gungor *et al.* [18], Kandlikar [21], and Wattelet *et al*. [12] correlations. Even though the correlations evolved for specific pure fluids or mixtures might not successfully predict for other new fluids, the one which predicts closer could be selected for further modification to suit this working fluid. It is also needless to say that some of the well known correlations [9, 10] are modified versions of correlations evolved for other fluids.

Test facility

The layout of the experimental test rig is shown in fig. 1a and 1b. The test facility consists of three circuits which are: the M09 circuit, the acetone circuit to heat the M09, and the auxiliary cooling circuit to condense the M09. The entire test section is constructed using hardened copper tube. The inner tube of the test section is 9.52 mm in diameter with 1.02 mm thickness and the outer tube diameter is 28.58 mm with 1.21 mm thickness. The test section is split in to 20 small sub section of 0.5 m length (only two sub sections are shown in fig. 1b). At the beginning of every subsection, the acetone temperatures (T_A) and outer wall temperature of the inner tube (T_{WO}) carrying M09 are measured using PT100 RTD sensors (accuracy of ±0.15 °C). Since the considered mixture is zeotropic in nature, at every section of the inner tube, the temperature was measured at the top and bottom (at south and north positions) as shown in fig. 1b. The average of

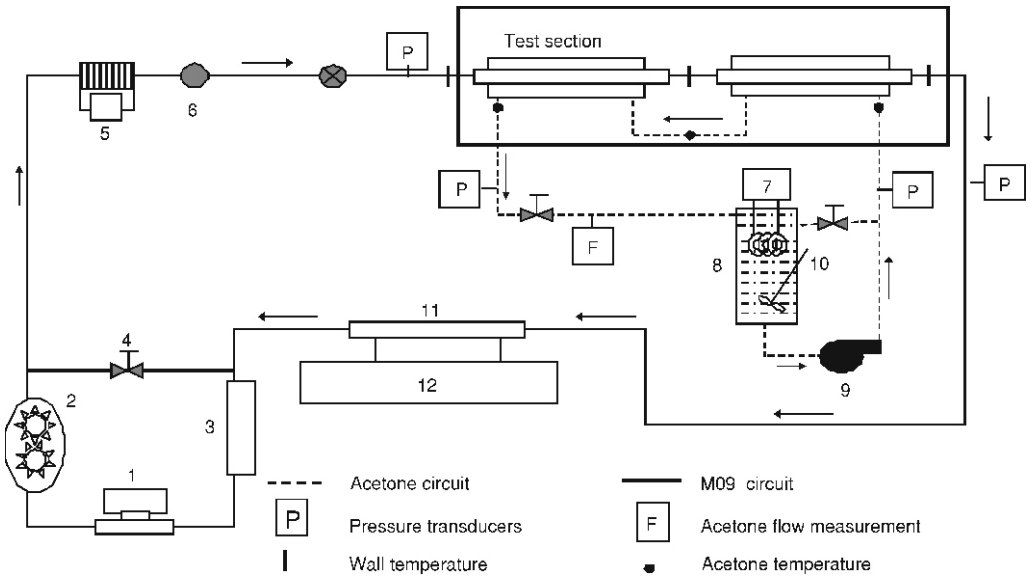

Figure 1a. Schematic layout of the experimental set up

1 – corriolis mass flow meter, 2 – magnetically coupled gear pump, 3 – liquid receiver, 4 – by-pass valve, 5 – pre-heater, 6 – sight glass, 7 – temperature controller, 8 – hot bath, 9 – acetone pump, 10 – stirrer, 11 – tube-in-tube condenser, 12 – auxiliary condensing unit

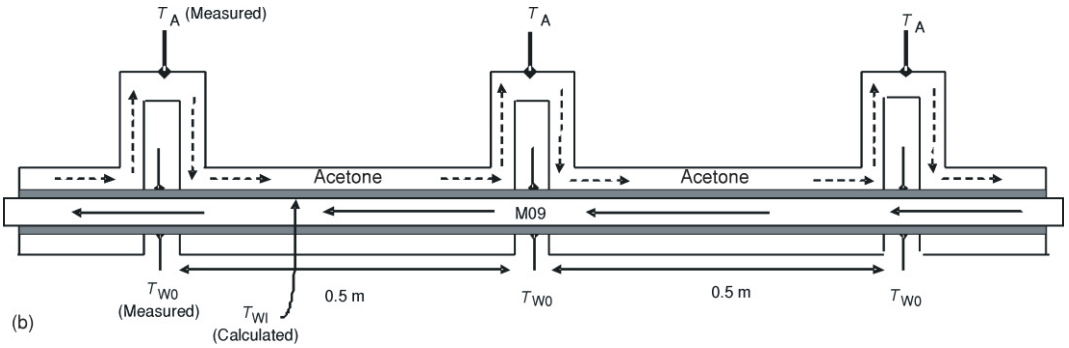

Figure 1b. Schematic view of a part of the test section

these two temperatures is considered as T_{WO}. The temperatures at various locations are recorded using a data acquisition system. The entire test section is effectively insulated with thermorex foam, thermocole, and glass wool. Based on the heat infiltration study it is seen that the maximum heat gain is 10.6 W/m^{2}K with respect to the outer surface area of the outer tube.

The M09 is pumped to the inlet of the test section (with 1 to 4 °C of sub-cooling) using a magnetically coupled sealess gear pump and it is boiled by the hot acetone which flows in counter-current direction. The vaporized M09 is then condensed back to a liquid receiver using an auxiliary condensing unit. The liquid is pumped back from the receiver to the test section via a mass flow meter. The cold acetone leaving the test section flows into a temperature controlled bath where the acetone is heated and pumped back to the test section using a magnetically coupled centrifugal pump. The M09 is metered using a Corriolis mass flow meter with ±0.1% accuracy. The pressure of the M09 is measured at the ends of the test section using an absolute piezo-resistive transducer with ±0.1% accuracy. The PT100 thin film temperature detectors are used to measure temperature at all necessary points. Acetone is metered using a suitable glass tube rota-meter with ±0.5% accuracy. An electric pre-heater of 100 W is provided at the inlet of the test section to regulate the entry condition of M09.

Table 1. Operating conditions for experimentation

Parameters	Range
$\dot{m}_R$ [g/s]	3 to 5
p_R [bar]	3.5 to 5
T_A [°C]	10 to 25
$\dot{m}_A$ [g/s]	55 to 75

Parameters fixed during tests are pressure of M09, mass flow rate of M09, mass flow rate of acetone, and inlet temperature of acetone. Using manufacturer's catalogue the mass flow rates prevailing in commercial refrigerators are estimated and the operating conditions are selected as shown in tab. 1. Once steady-state conditions are achieved, the signals from pressure transducers, mass flow meter, and temperature sensors are logged into the data logger. Multiple trials of data logging is performed for a fixed interval of time and stored in spread sheets. The heat transfer coefficients are then deduced by dynamically linking a MATLAB program and spreadsheets.

Data reduction

The reported heat transfer coefficients are average heat transfer coefficient of every subsections. The tube wall temperatures (T_{WO}), acetone temperature (T_A) , pressure at the inlet and the exit of the test section (p_R), mass flow rate of M09 ($\dot{m}_R$), and acetone mass flow rate ($\dot{m}_A$) are the observed data. The actual location of incipience and completion of saturated boiling of M09 in the test section is not known directly. Hence the acetone temperature distribution is fit against the length of the test section as a polynomial. Considering this temperature variation for the heat input and based on the inlet condition, saturation condition, and the latent heat of evaporation of the M09, the entire length of the test section is divided into sub-cooled, two phase and super heated length. Sub-cooled length is estimated by equating the acetone heat load to the sub-cooled load of the M09 as shown in eq. 1. Further, the acetone heat load is interactively balanced [23] against the latent heat of vaporization ($\dot{m}_R \Delta i_{fg}$) along the length of the test section. This gives vapour quality $x = f(p - \Delta p , h_f + \Delta i_{fg})$ and M09 equilibrium temperature for a given vapour quality $T_R = f(p - \Delta p, x)$ at the end of every sub section. The length after $x = 1$ is the superheated length which is not considered for the study.

The pressures are measured only at the inlet and outlet of the test section. Since the pressure drop is negligible in a low mass flow rate application, a linear variation of pressure drop is assumed along the test section. Considering the heat flux, the Fourier radial heat conduction

equation and the measured outer wall temperature (T_{WO}), the inner tube wall temperature (T_{WI}) can be calculated using eq. 2 . Finally the heat transfer coefficients can be evaluated using eq. 3. REFPROP [24] is used to estimate the thermo-physical properties of both the fluids.

$$(\Delta L)_{SUB} \quad \frac{\dot{m}_R Cp_R (T_{BUB} \quad T_{SUB})}{\dot{m}_A Cp_A \quad \frac{\partial T}{\partial L}_A} \tag{1}$$

$$T_{WI} \quad T_{WO} \quad \frac{q_{SEG} \ln \frac{D_O}{D_I}}{2\pi k (\Delta L)_{SEG}} \tag{2}$$

$$h_R \quad \frac{q_{SEG}}{(T_{WI} \quad T_R)} \tag{3}$$

Experimental set up validation

The error analysis for the heat transfer coefficient is carried out by applying the uncertainty analysis suggested in published literature [25].The input to the heat transfer coefficient is the heat flux (q) and the wall super heat. In this counter-current heat exchanger the heat flux (q) depends on mass flow rate ($\dot{m}_A$) and temperature difference of acetone. The overall uncertainty in estimating h_R is found to be within ±30.31 to ±60.67 W/m^{2}K. To check the repeatability of the experimental set up, tests are performed as prescribed in Ross *et al.* [15]. The repeatability test is conducted for the lowest mass flow rate of 3.5 g/s at 3.5 bar and the deviation of heat transfer coefficient is within in ±1.5% only. The test section was validated with R-134a before conducting experiments with M09. The results were compared with experimental data of Wattelet *et al*. [12] which was evolved with similar conditions and the average deviation is found to be within ±7% only.

Results and discussion

The experiment was conducted for the range of operating conditions mentioned in tab. 1. Around 1404 data points have been obtained through the experiments. It is known that the flow pattern of the flowing refrigerant inside the tube significantly influences heat transfer coefficient. Flow pattern map, a tool to predict the flow patterns has been reported in Thome [22]. A similar flow pattern map, as shown in fig. 2, is constructed for M09 for the different operating pressures considered. Figure 2 is specific to 4 bar at which the heat fluxes viz 1, 5, and 9 kW/m^2 are considered. At 4 bar for the mass

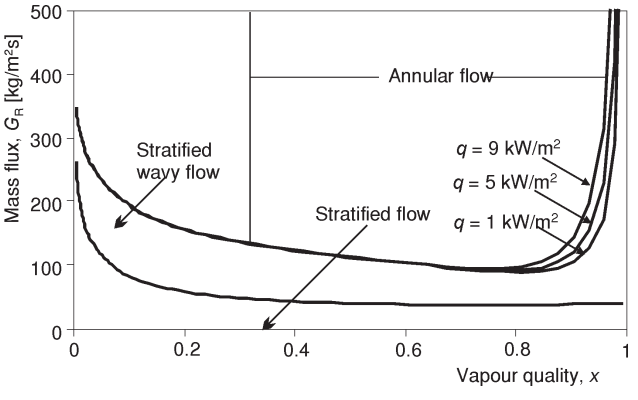

Figure 2. Flow pattern map of M09 mixture at 4 bar

flow rate ($\dot{m}_R$) ranging from 3 to 5 g/s, the mass flux (G_R) is varied between 68 to 113 kg/m^{2}s. It is observed that the predominant flow patterns are stratified and stratified-wavy pattern.

The distribution of the T_{WO}, T_A, T_R, and x along the length of the test section is shown in fig. 3. As described earlier, the M09 is pumped into the test section in a sub-cooled state. Hence a portion of the test section will have sensible heat transfer to liquid M09 till it reaches its bubble temperature (T_{BUB}). It is observed that for the considered flow conditions the M09 completely vaporizes at around 6 m and the sub-cooled length is calculated to be 0.24 m. The remaining length of 4 m is the super heating length. These lengths are estimated by balancing the acetone heat load with enthalpy change in M09 as described in the data reduction section. The glide experienced in T_R including the effect of a pressure drop is 5.92 °C (theoretical glide from REFPROP is 6.45 °C, T_{BUB} = –1.8 °C to T_{DEW} = 4.65 °C).

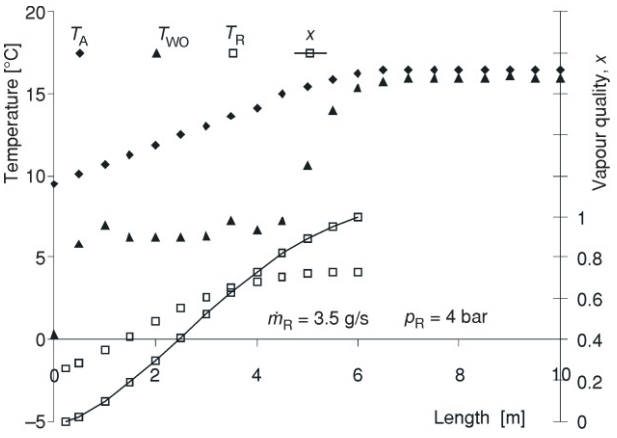

Figure 3. Temperature distribution along the length of the test section

As mentioned earlier, in a counter-current heat exchanger test section, the local heat flux varies along the length. This is exhibited in fig. 4 for a constant acetone inlet condition and refrigerant pressure (p_R) of 4 bar and different M09 mass flow rates ($\dot{m}_R$). It can be seen that heat flux during incipience of boiling is higher for low flow rates. This is because at lower flow rate ($\dot{m}_R$ = 3.0 g/s) the nucleation resistance is low and the boiling occurs rapidly than at higher flow rate ($\dot{m}_R$ = 5.0 g/s). This high level of flashing at low $\dot{m}_R$ results in higher heat flux being taken from the acetone.

However, in later part of the tube there will not be sufficient liquid (M09) in the test section to sustain the same heat flux. But at higher flow rate $\dot{m}_R$ = 5 g/s, due to increased nucleation resistance by the flow velocity in the initial stage of boiling, the heat flux starts with a low value. However as the flow proceeds due to increased vapor velocity of the M09, the heat flux increases due to convective vaporization. In the later part of the tube, the heat flux rapidly decreases due to deficiency of liquid M09. It is seen that the two phase length increases as the mass flow rate increases. The initial heat flux is maximum for the lowest flow rate and the heat flux at the end is maximum for the highest flow rate condition. Thus the transport properties are dependent on the flow rate irrespective of the load.

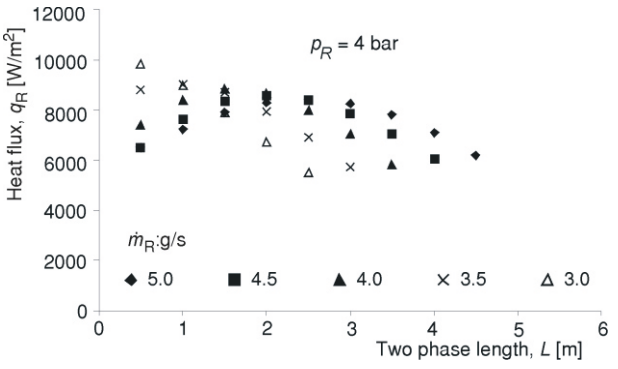

Figure 4. Influence of heat flux on two phase length

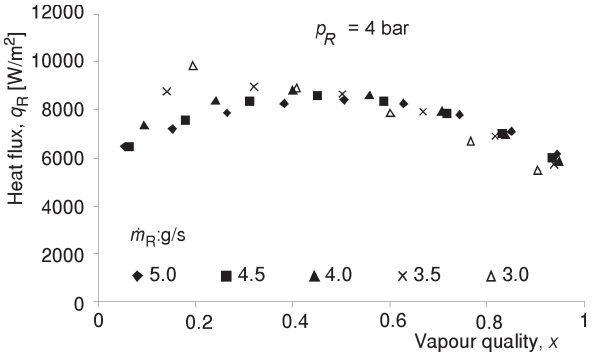

Figure 5. Variation of heat flux with respect to dryness fraction

The variation of heat flux against vapour quality for different flow rate is shown in fig. 5. It can be noted that even though the two phase length is decided by $\dot{m}_R$, irrespective of the flow rate the heat flux realized tends to converge above a vapour quality say 0.5. This implies that the increased convective effect due to higher mass flow rate has not dominated in the higher vapour quality regions unlike annular flow. Thus in stratified and stratified-wavy flow the nucleation mechanism continues to prevail even at higher vapour quality zones. Due to practical difficulty, heat flux is mostly considered as a primary input variable along with pressure and mass flow rate. But the above discussion evinces that heat flux itself is a coupled function of pressure and mass flow rate. Hence it is more realistic to formulate the heat transfer correlation with pressure and mass flow rate of the refrigerant as independent parameters and heat flux as a dependent parameter.

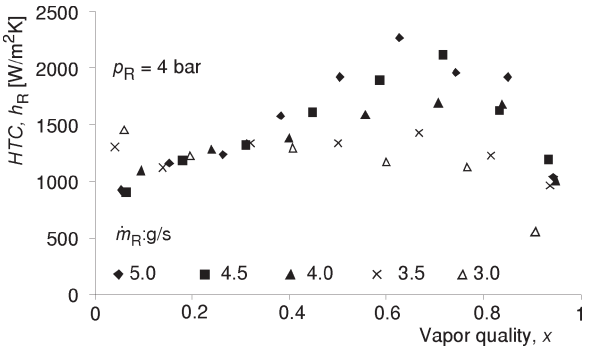

Figure 6. Influence of mass flow rate on heat transfer coefficient

The variation of heat transfer coefficient against vapour quality is shown in fig. 6. It is seen that at lower flow rates ($\dot{m}_R$) higher rate of nucleation causes a rapid removal of heat from the surface, which results in a sudden drop in inner wall temperature and hence the wall super heat also decreases. The observed trend of heat transfer coefficient with respect to vapour quality is due to higher nucleation in the beginning which subsides as the vapor fraction increases and the convective heat transfer compensates to some extent due to increased vapor velocity. It should be noted in fig. 2 that when $\dot{m}_R$ = 5.0 g/s and vapour quality ranging between 0.6 to 0.85, the flow enters into annular region .This results in a high heat transfer coefficient. The peak heat transfer coefficient realized at 3.0-5.0 g/s lies between 1.25 and 2.2 kW/m^{2}K. As discussed in Aprea *et al*. [14], it can be noted that in a low mass flow rate condition, the convective effects are less dominant in the low quality regions. However the convective effects try to dominate at moderate vapour qualities (around 0.6 to 0.8). This increase in heat transfer coefficient realized even when the heat flux rise is marginal can be attributed to the reduction in wall superheat due to the experienced temperature glide.

The variation of heat transfer coefficient against vapour quality for a constant pressure and mass flow rate for different level of mean heat flux is shown in figs. 7a and 7b. It is known that in an annular flow, for a constant pressure and mass flow rate, the heat transfer coefficient is independent of heat flux once the nucleations are suppressed. Further the heat transfer coefficient lines will tend to merge in to single line [9-13] after the point of suppression. But in the

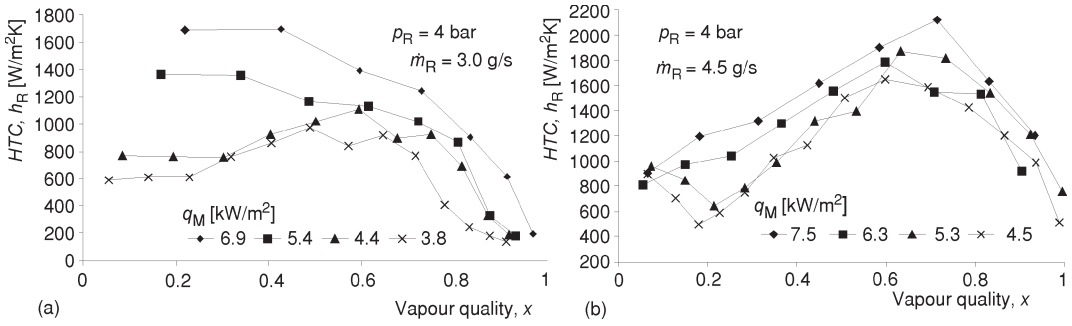

Figure 7. Influence of heat flux on heat transfer coefficient at (a) $\dot{m}_R$ = 3.0 g/s and (b) $\dot{m}_R$ = 4.5 g/s

case of stratified-wavy flow it can be seen that lines does not merge completely which indicates that the heat transfer coefficient continues to be a function of heat flux even at higher dryness fraction. However the trend indicates that the difference in heat transfer coefficient decreases as vapour quality increases.

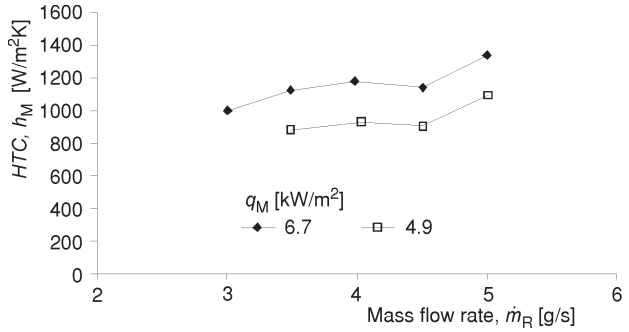

Figure 8. Mean heat transfer coefficient as a function of mass flow rate

Figure 8 shows the variation of mean heat transfer coefficient against mass flow rate at different heat flux conditions. It is obvious that when the mass flux is increased, the average *HTC* will increase proportionate to the extent to which convective vaporization is established. In the present case until 4.5 g/s the nucleation component dominates and the curve is not steep. However beyond 4.5 g/s, the increased mass flow rate enables convective component to dominate over nucleation and the heat transfer coefficient increases at a faster rate.

The impact of pressure on the heat transfer coefficients for the same heat load condition is shown in fig. 9a and 9b. For a given mass flow rate (say 3.5 g/s) as pressure increases the

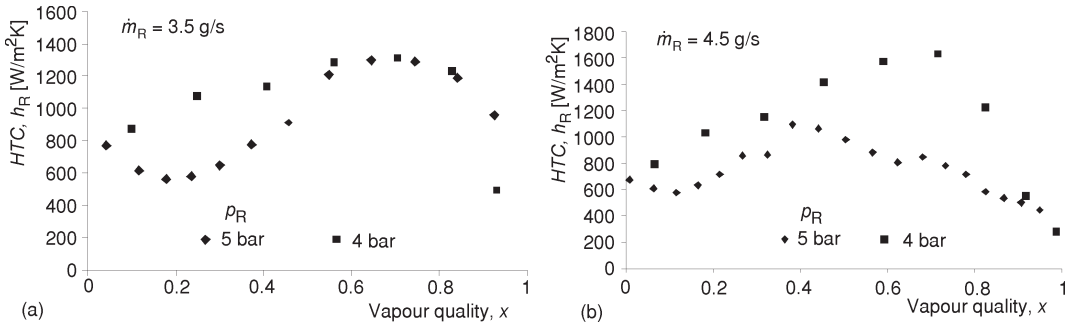

Figure 9. Influence of pressure on heat transfer coefficient at (a) $\dot{m}_R$ = 3.5 g/s and (b) $\dot{m}_R$ = 4.5 g/s

heat transfer coefficient decreases. The rise in pressure causes the saturation temperature to rise leading to a drop in wall superheat that impedes the nucleation rate. However if the flow is predominantly annular the rise in pressure would favour the heat transfer coefficient as it is more influenced by the convective effects than nucleation effects [9-13]. Thus it is inferred that the nucleation effects prevail over convective effects in the region of stratified and stratified-wavy flow pattern irrespective of pressure. This has to be considered when correlations are evolved to get better prediction. Jabardo *et al.* [13] also reported the same phenomenon claiming that the conductivity of the liquid diminishes with temperature and so does the heat transfer coefficient.

Hence it can be concluded that irrespective of vapour quality the heat transfer coefficient is a function of pressure, mass flow rate and the heat flux.

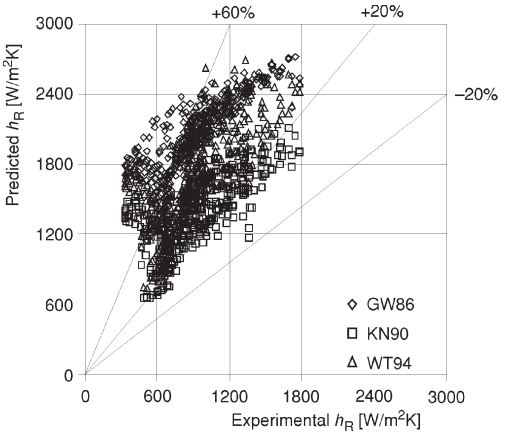

Figure 10. Deviation plot for heat transfer coefficients

In the absence of an exclusive correlation for the considered mixture, a comparison of the experimental results with prediction based on familiar correlations for other pure fluids or mixtures is not unusual [14]. Hence the experimentally evolved heat transfer coefficient values of M09 are compared with correlations. This would help in identifying a correlation (from existing correlations) that closely predicts the heat transfer coefficient of the present mixture and the same correlation can be considered for suitable modification to improve the accuracy. A comparison of experimental heat transfer coefficient with that predicted by correlations such as Gungor *et al.* [18], Kandlikar [21], and Wattelet *et al*. [12] marked as GW86, KN90, and WT94, respectively, is shown in fig. 10.

The Kandlikar correlation requires a fluid dependent number (*Fl*) for M09, which is not readily available. The value of R-134a (*Fl* = 1.63), which is also 91% of the mixture, is considered for Kandlikar correlation. It is found that the predictions of these correlations are mostly scattered between +60% and –20% deviation. It is to be noted that these correlations predict with reasonable accuracy for high flow rates where annular flow prevails. Hence it is necessary to evolve a suitable correlation for M09 applicable to stratified and stratified-wavy flow regimes which will be published in the future.

Most of the pioneering flow boiling heat transfer experiments have used energy balance between the fluid mediums to estimate the heat transfer coefficient. However, the relation between the heat transfer coefficient and the dryness fraction in a stratified flow can be best exploited by direct measurement of void fraction. This dynamic void fraction measurement method, called as optical image processing analysis technique [26], can also record the accurate flow pattern for a particular operating condition. Thus the vital information such as liquid film thickness, wetted perimeter, liquid – vapour interface perimeter etc., can also be extracted in order to improve the accuracy of a correlation.

Conclusions

Experiments on M09 (R-134a/R-290/R-600a: 91%/4.068%/4.932% by mass) performed at low mass flow rates revealed that nucleation effects are present even at high vapor quality. It is ob-

served that for a low mass flow rates ($\dot{m}_R$) of 3 to 5 g/s and heat flux of 2 to 8 kW/m^2, the heat transfer coefficient is estimated to be falling between 500 to 2200 W/m^{2}K. The results also indicate that in stratified and stratified-wavy flow, the *HTC*s are dependent on heat flux even at moderate qualities when pressure (p_R) and mass flow rate ($\dot{m}_R$) are kept constant. It is found that the predicted heat transfer coefficient using familiar correlation are scattered between +60% and –20% deviation.

Acknowledgment

The authors acknowledge the grant-in-aid provided by Department of Science and Technology (DST-SERC), India for conducting the study. Project reference number: SR/S3/MERC/61/2004-SERC-Engg.

Nomenclature

- A – cross-section area, [m^{-2}]
- Cp – specific heat capacity, [Jkg^{-1}K^{-1}]
- D – diameter of inner tube, [m]
- Fl – fluid dependent parameter, [–]
- G – mass flux (= $\dot{m}/A$), [kgm^{-2}s^{-1}]
- g – acceleration due to gravity, [ms^{-2}]
- h, HTC – heat transfer coefficients, [Wm^{-2}K^{-1}]
- i – enthalpy, [Jkg^{-1}]
- k – copper thermal conductivity, [Wm^{-1}K^{-1}]
- L – length, [m]
- m – mass flow rate, [gs^{-1}]
- p – pressure [bar]
- q – heat flux, [Wm^{-2}]
- T – temperature, [K], [°C]
- x – vapour quality, [–]

Greek symbols

- Δ – differential
- μ – liquid viscosity [Pa·s]

Subscripts

- A – acetone
- BUB – bubble point
- DEW – dew point
- fg – latent heat
- I – inner side, inner tube
- M – mean values
- O – outer side
- R – local M09 condition
- SAT – saturation
- SEG – segmental
- SUB – sub-cooled
- TP – two phase
- WI – inside wall of inner tube
- WO – outside wall of inner tube

References

[1] ***, United Nations Environment Programme, Montreal Protocol on Substances that Deplete the Ozone Layer. Final Act, 1989
[2] Devotta, S., Gopichand, S., Comparative Assessment of HFC134a and Some Refrigerants as Alternatives to CFC12, *Int. J. Refrigeration, 15* (1992), 2, pp. 112-118
[3] Devotta, S., Parande, M. G., Patwardhan, V. R., Performance and Heat Transfer Characteristics of HFC-134a and CFC-12 in a Water Chiller, *Applied Thermal Engg., 18* (1998), 7, pp. 569-578
[4] Jung, D., Kim, C. B., Lim, B. H., Lee, H.W., Testing of a Hydrocarbon Mixture in Domestic Refrigerators, ASHRAE Trans. 1996, pp. 1077-1184
[5] Fatouh, M., El Kafafy, M., Assessment of Propane/Commercial Butane Mixtures as Possible Alternatives to R134a in Domestic Refrigerators, *Energy Conversion and Management, 47* (2006), 15-16, pp. 2644-2658
[6] Sekhar, S. J., Kumar, K. S., Lal, D. M., Ozone Friendly HFC134a/HC Mixture Compatible with Mineral Oil in Refrigeration System Improves Energy Efficiency of a Walk in Cooler, *Energy Conversion and Management, 45* (2004), 7-8, pp. 1175-1186
[7] Sekhar, S. J., Premnath, R. P., Lal, D. M., On the Performance of HFC134a/HC600a/HC290 Mixture in a CFC12 Compressor with Mineral Oil as Lubricant, *EcoLibrium* – Journal of Australian Institute of Refrigeration, Air Conditioning and Heating, *2* (2003), 4, pp. 24-29

[8] Chen, J. C., Correlation for Boiling Heat Transfer to Saturated Fluids in Convective Flow, *Industrial and Engineering Chemistry Process Design and Development, 5* (1966), 3, pp. 322-329
[9] Jung, D. S., *et al*., A Study of Flow Boiling Heat Transfer with Refrigerant Mixtures, *Int. J. of Heat and Mass Transfer, 32* (1989), 9, pp. 1751-1764
[10] Jung, D. S., *et al.*, Horizontal Flow Boiling Heat Transfer Experiments with a Mixture of R22/R114, *Int. J. Heat Mass Transfer, 32* (1989), 9, pp. 131-145
[11] Shin, J. Y., Kim, M. S., Ro, S. T., Experimental Study on Forced Convective Boiling Heat Transfer of Pure Refrigerants and Refrigerant Mixtures in a Horizontal Tube, *Int. J. Refrigeration, 20* (1997), 4, pp. 267-275
[12] Wattelet, J. P., *et al*., Evaporative Characteristics of R12, R134a and a Mixture at Low Mass Fluxes, *ASHRAE Trans. Symposia, 2* (1994), 1, pp. 603-615
[13] Jabardo, J. M. S., Filho, E. P. B., Convective Boiling of Halocarbon Refrigerants Flowing in a Horizontal Copper Tube an Experimental Study, *Thermal and Fluid Science, 23* (2000), 3, pp. 93-104
[14] Aprea, C., Rossi, F., Greco, A., Experimental Evaluation of R22 and R407C Evaporative Heat Transfer Coefficient in a Vapour Compression Plant, *Int. J. Refrigeration, 23* (2000), 5, pp. 366-377
[15] Ross, H., *et al*., Horizontal Flow Boiling of Pure and Mixed Refrigerants, *Int. J. Heat Mass Transfer, 30* (1987), 5, pp. 979-992
[16] Kattan, N., Thome, J. R., Favrat, D., Flow Boiling in Horizontal Tubes: Part 1 – Development of a Diabatic Two-Phase Flow Pattern Map, *J. of Heat Transfer, 120* (1998), 1, pp. 140-147
[17] Kattan, N., Thome, J. R., Favrat, D., Flow Boiling in Horizontal Tubes: Part 3 – Development of a New Heat Transfer Model Based on Flow Pattern, *J. of Heat Transfer, 120* (1998), 1, pp. 156-165
[18] Gungor, K. E., Winterton, R. H. S., A General Correlation for Flow Boiling in Tubes and Annuli, *Int. J. Heat Mass Transfer, 29* (1986), 3, pp. 351-358
[19] Gungor, K. E., Winterton, R. H. S., Simplified General Correlation for Saturated Flow Boiling and Comparisons of Correlations with Data, *Chem. Eng Res. Des., 65* (1987), March, pp. 148-156
[20] Shah, M. M., Chart Correlation for Saturated Boiling Heat Transfer: Equations and Further Study, *ASHRAE Transaction, 88* (1982), 1, pp. 185-196
[21] Kandlikar, S. G., A General Correlation for Saturated Two-Phase Flow Boiling Heat Transfer Inside Horizontal and Vertical Tubes, *J. of Heat Transfer, 112* (1990), 1, pp. 219-228
[22] Thome, J. R., Update on Advances in Flow Pattern Based Two-Phase Heat Transfer Models, *Experimental Thermal and Fluid Science, 29* (2005), 3, pp. 341-349
[23] Boissieux, X., Heikal, M. R., Johns, R. A., Two-Phase Heat Transfer Coefficient of Three HFC Refrigerants Inside a Horizontal Smooth Tube, Part I: Evaporation, *Int. J. of Refrigeration, 23* (2000), 4, pp. 269-283
[24] ***, REFPROP, NIST Standard Reference Database 23, Version 7.01, 2004
[25] Moffat, R. J., Describing the Uncertainties in Experimental Results, *Experimental Thermal and Fluid Science, 1* (1988), 3, pp. 3-17
[26] Wojtan, L., Ursenbacher, T., Thome, J. R., Measurement of Dynamic Void Fractions in Stratified Types of Flow, *Experimental Thermal and Fluid Science, 29* (2005), 3, pp. 383-392

Author's address:

B. Raja, D. Mohan Lal, R. Saravanan
Department of Mechanical Engineering,
College of Engineering, Guindy, Anna University
Chennai – 600 025, India

Corresponding author B. Raja
E-mail: raja_cfd@yahoo.com

Paper submitted: December 21, 2007
Paper revised: February 28, 2008
Paper accepted: March 12, 2008